Molecular Crystals and Liquid Crystals
Publication details, including instructions for authors and subscription information:
http://www.tandfonline.com/loi/gmcl16

Chemistry of Binary and Ternary Organic Eutectics

R. P. Rastogi [a] , D. P. Singh [a] , Namwar Singh [a] & Narsingh Bahadur Singh [b]

[a] Chemistry Department, Gorakhpur University, Gorakhpur, (U.P.), India

[b] Materials Engineering Departments, Rensselaer Polytechnic Institute, Troy, New York, 12181, U.S.A.

Version of record first published: 20 Apr 2011.

To cite this article: R. P. Rastogi , D. P. Singh , Namwar Singh & Narsingh Bahadur Singh (1981): Chemistry of Binary and Ternary Organic Eutectics, Molecular Crystals and Liquid Crystals, 73:1-2, 7-34

To link to this article: http://dx.doi.org/10.1080/00268948108076259

Mol. Cryst. Liq. Cryst., 1981, Vol. 73, pp. 7–34
0026-8941/81/7302–0007 $06.50/0

Printed in the United States of America

Chemistry of Binary and Ternary Organic Eutectics

R. P. RASTOGI, D. P. SINGH and NAMWAR SINGH
Chemistry Department, Gorakhpur University, Gorakhpur (U.P.) India

and

NARSINGH BAHADUR SINGH†
Materials Engineering Departments, Rensselaer Polytechnic Institute, Troy, New York 12181 U.S.A.

(*Received May 4, 1981*)

With a view to elucidate the chemistry of binary and ternary organic eutectics, we measured phase diagrams, undercooling and linear velocity of crystallization of molten mixtures of α·naphthol-*m*·aminophenol, α·naphthol-phenathrene, β·naphthol-phenanthrene, β·naphthol-*m*·aminophenol, α·naphthol-β·naphthol-catechol, α·naphthol-catechol-naphthalene, α·naphthol-β·naphthol-phenanthrene and α·naphthol-β·naphthol-*m*·aminophenol systems. Microscopic studies and heat of fusion measurements were made to investigate the characteristics of the eutectics. The heats of fusion data do not obey the mixture law. The excess thermodynamic functions such as g^E, h^E and s^E were also computed for the binary systems. Microscopic studies showed that freshly precipitated eutectics have different characteristics as compared to parent components. The growth rates are analyzed using the current theories of crystallization and a mechanism of growth has been proposed for the binary and ternary eutectics.

INTRODUCTION

Considerable advances have been made in the past few years in the knowledge of growth behavior of eutectics,[1–5] by using the techniques developed and the understanding gained from single phase solidification. Generally the growth morphology of eutectics depends on the growth characteristics of individual constituent phases. The constituent phases can solidify either with faceted or

† Address for Correspondence

with non-faceted interfaces. This behavior is related to the nature of solid–liquid interface and can be predicted for pure materials from the entropy of fusion. Organic compounds are being widely used as model substances for crystal growth process. They have the advantages of transparency and low transformation temperture, allowing the direct observation of crystallization process.

Ternary organic eutectics have not been studied in detail. In the present paper the following binary and ternary systems were chosen.

α · naphthol-*m* · aminophenol
β · naphthol-*m* · aminophenol
α · naphthol-phenanthrene
β · naphthol-phenanthrene
α · naphthol-catechol-naphthalene
α · naphthol-β · naphthol-catechol
α · naphthol-β · naphthol-phenanthrene
α · naphthol-β · naphthol-*m* · aminophenol.

These eutectics were studied for their microstructure, heat of fusion, undercooling, phase diagram and crystallization rate. The heat of fusion values are compared with the values predicted by an empirical formula. The excess thermodynamic functions such as g^E, h^E and s^E are also computed for the binary systems.

EXPERIMENTAL

The α · naphthol, β · naphthol, catechol and *m* · aminophenol were from BDH, Bombay, India. All of these were purified by repeated distillation under low pressure. Phenanthrene was distilled and further purified by fractional crystallization with ethyl alcohol. The purity of each sample was checked by determining the melting point. The melting points of the purified sample were 95.8, 122.0, 122.2, 104.2 and 100.0°C for α · naphthol, β · naphthol, *m* · aminophenol, catechol and phenanthrene, respectively. The values are in good agreement with literature values.

The phase diagrams were determined by the thaw-melt method.[6,7] Mixtures of different compositions were prepared in glass test tubes by repeated heating, chilling and grinding in a glass mortar. The thermometer used could be read to 0.1°C. The maximum undercooling was also determined by the method described in Ref. 8.

The linear velocity of crystallization was determined by using a method similar to that adopted by Singh and Singh.[9] Photomicrographs were taken of microscope slides of eutectics.[8]

Heats of fusion were measured with a double walled calorimeter. The temperature variation was recorded by a chromel-alumel thermocouple. The heat of fusion was calculated by

$$\Delta_f h = \frac{E \cdot I \cdot t \cdot M}{m} \tag{1}$$

where E is the voltage across the heater, I is the voltage across a standard resistance of one ohm, t is the time required for complete melting, M is molecular weight and m is the mass of the mixture.

RESULTS AND DISCUSSION

The phase diagrams are shown in Figures 1 to 4 for the binary systems. The projections of the ternary systems are plotted in Figures 5 thru 8. The point e_1, e_2 and e_3 are the binary eutectic points between the parent phases, and e and p are ternary eutectic and peritectic points.

The linear velocities of crystallization are recorded in Figures 9–12 as log V vs. log ΔT.

The microstructures of different eutectics are shown in Figures 13–26. The heats of fusion are shown in Table I, and compared with values calculated by a mixture law.

(a) Phase diagram and undercooling

The solid-liquid equilibrium data for the α·naphthol-*m*·aminophenol and β·naphthol-phenanthrene systems indicate that they form simple eutectics, while β·naphthol-*m*·aminophenol and α·naphthol-phenanthrene form 1:1 compounds with congruent melting points. The α·naphthol-β·naphthol-catechol and α·naphthol-catechol-naphthalene systems form simple ternary eutectics. The α·naphthol-β·naphthol-*m*·aminophenol and α·naphthol-β·naphthol-phenanthrene systems have one ternary eutectic and one ternary peritectic. The eutectic compositions for ternary systems were estimated by equation

$$\log X_i = -\frac{\Delta_f h_i (T_e - T_i^0)}{4.576\, T_e T_i} \tag{2}$$

and

$$X_1 + X_2 + X_3 = 1. \tag{3}$$

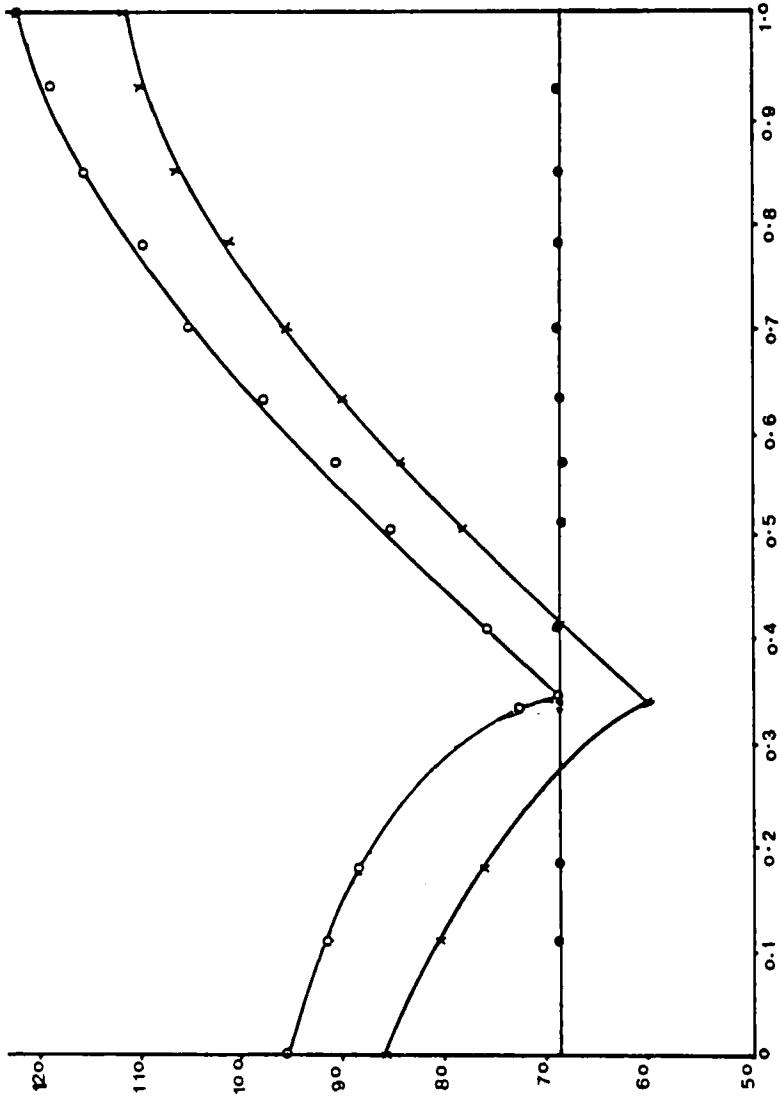

FIGURE 1 Phase Diagram of α-naphthol-*m*-aminophenol system: ⊙ Melting Points; ● Thaw points; × Temperature of spontaneous crystallization.

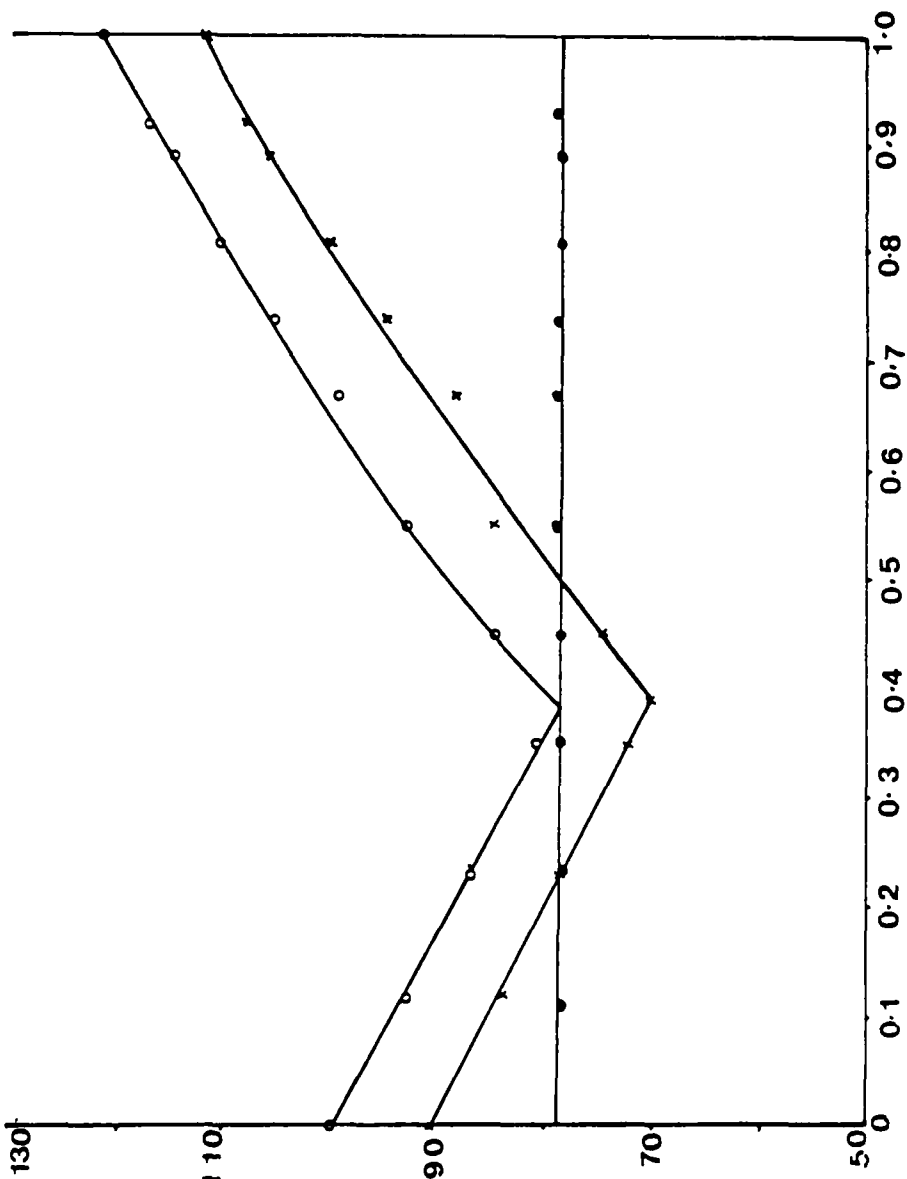

FIGURE 2 Phase Diagram of β-naphthol-phenanthrene system: ⊙ Melting Points; ● Thaw points; × Temperature of spontaneous crystallization.

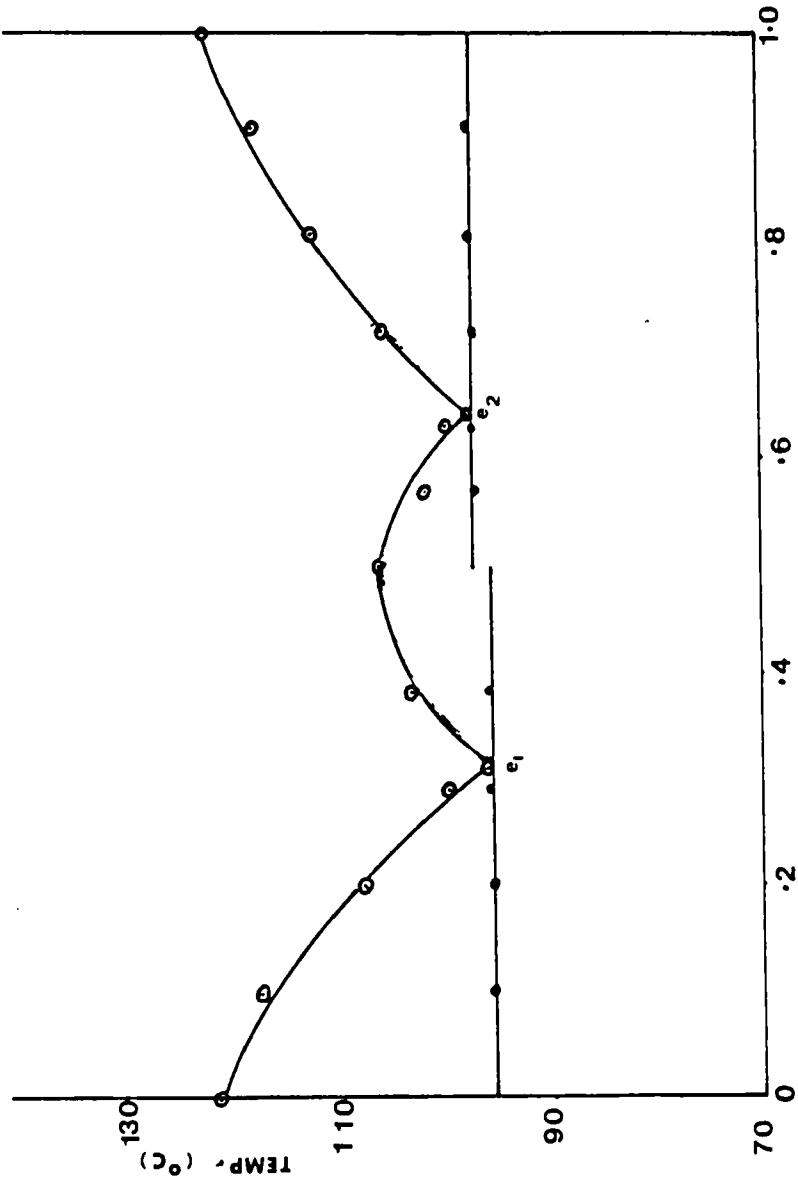

FIGURE 3 Phase Diagram of β-naphthol-*m*-aminophenol system: ⊙ Melting Points; ● Thaw points.

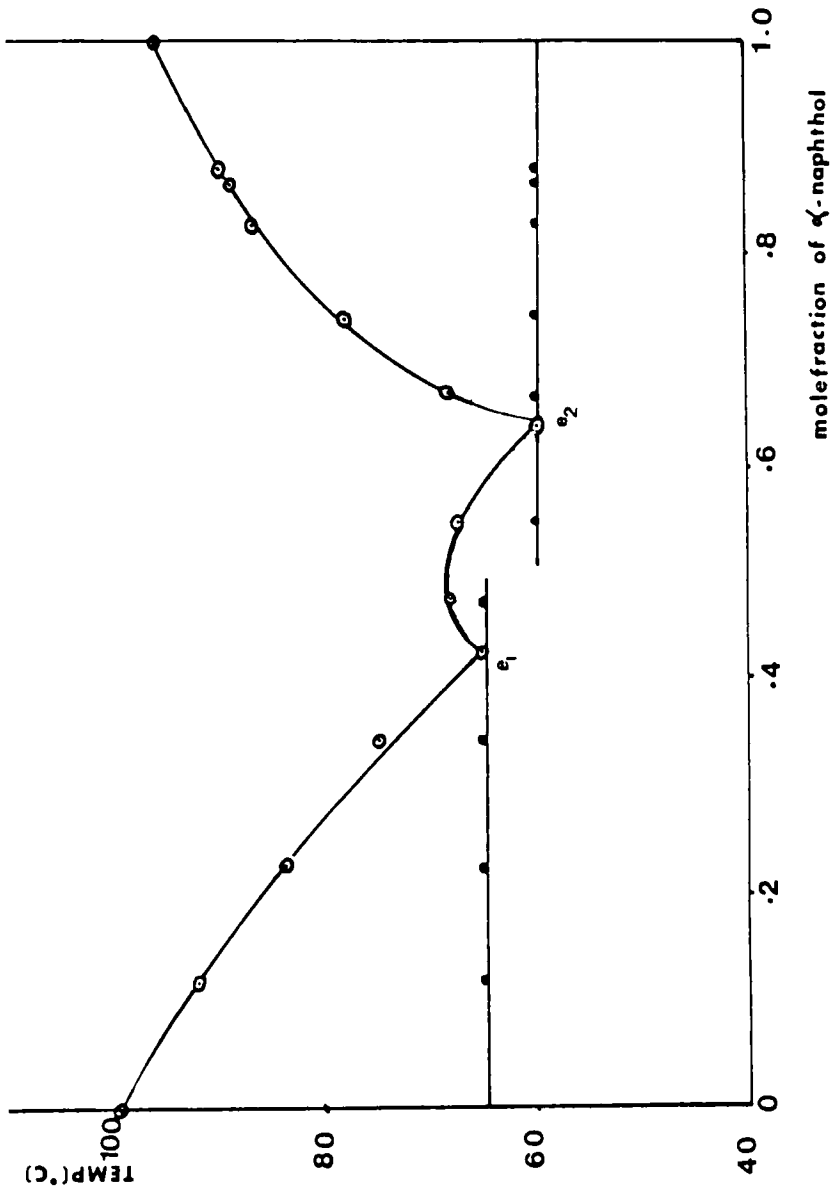

FIGURE 4 Phase Diagram of α-naphthol-phenanthrene system: ⊙ Melting Points; ● Thaw points.

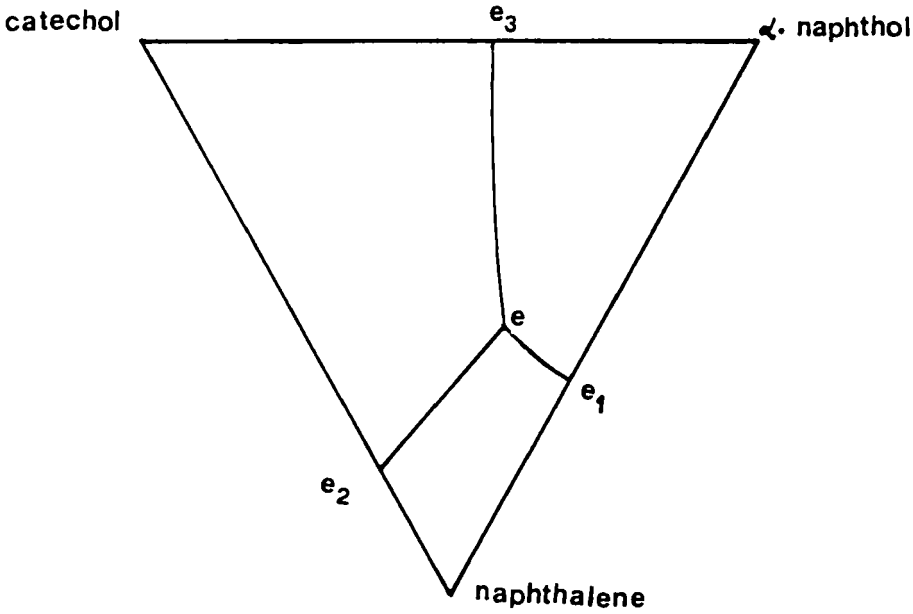

FIGURE 5 Projection of Phase Diagram of naphthalene-α·naphthol-catechol-*m*·amino-phenol System.

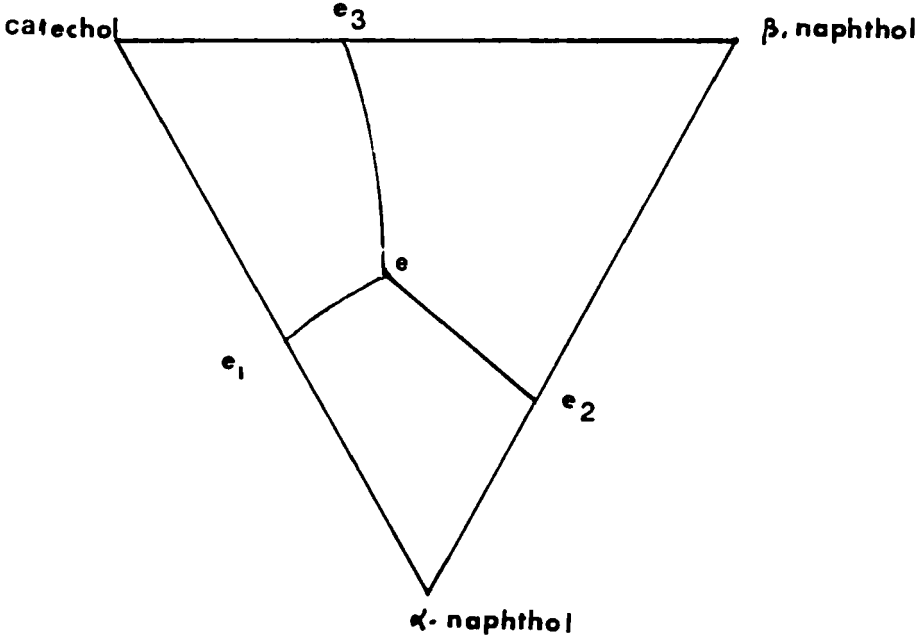

FIGURE 6 Projection of Phase Diagram of α·naphthol-β·naphthol-cathechol System.

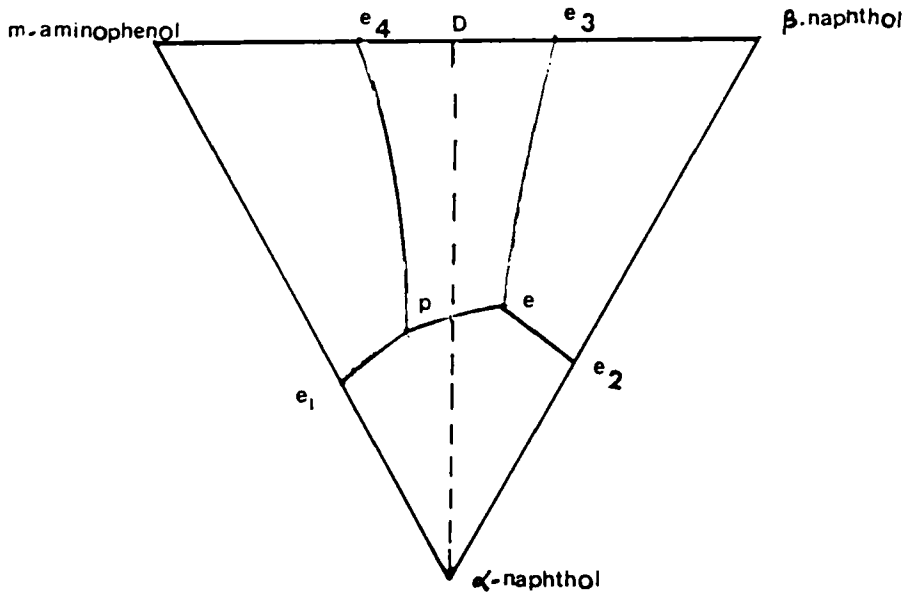

FIGURE 7 Projection of Phase Diagram of α · naphthol-β · naphthol-m · aminophenol System.

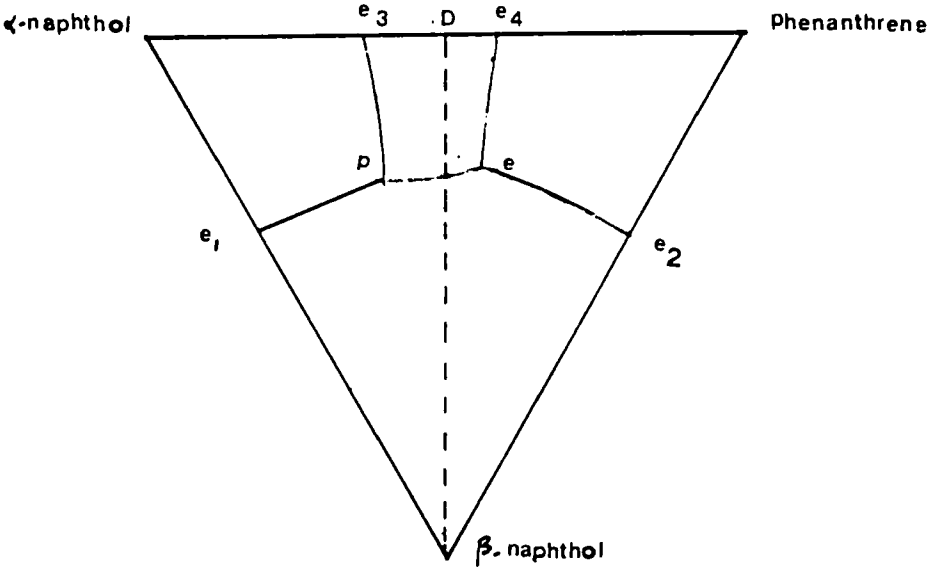

FIGURE 8 Projection of Phase Diagram of α · naphthol-β · naphthol-phenathrene System.

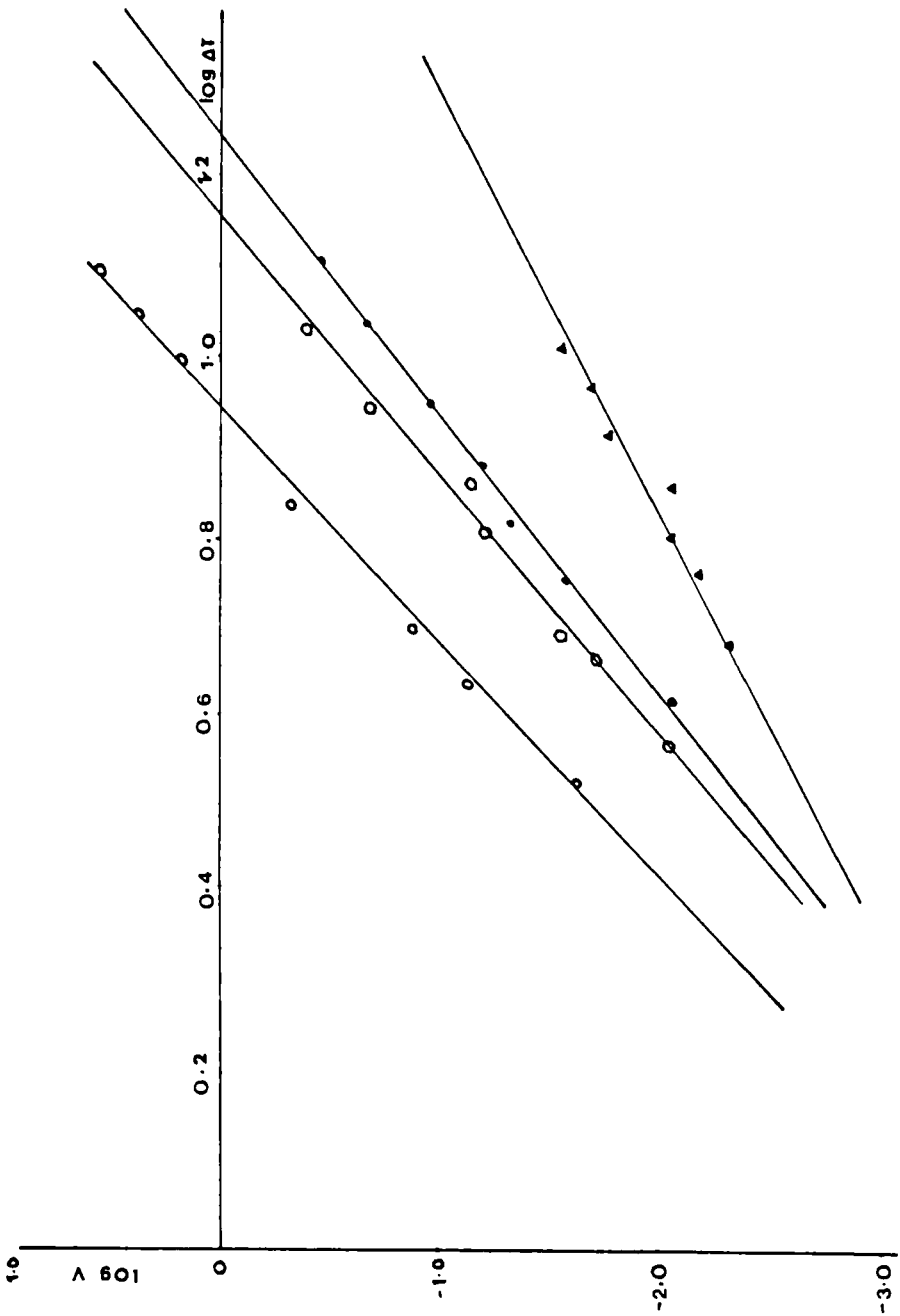

FIGURE 9 Linear Velocity of Crystallization of α · naphthol-β · naphthol-catechol System. ○ β · naphthol; ○ α · naphthol; ● catechol; ▲ ternary eutectic.

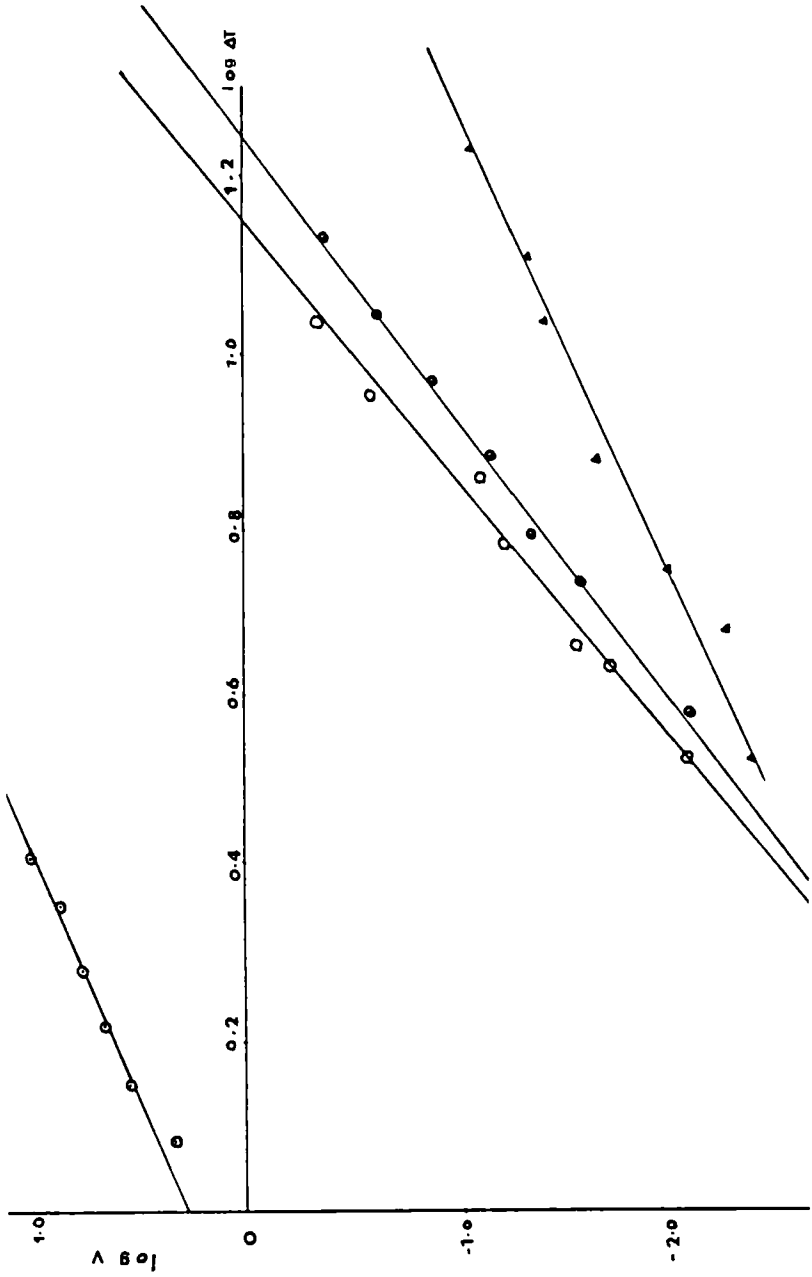

FIGURE 10 Linear Velocity of Crystallization of naphthalene-α·naphthol-catechol System. O α·naphthol; ⊙ naphthalene; ● catechol; ▲ ternary eutectic.

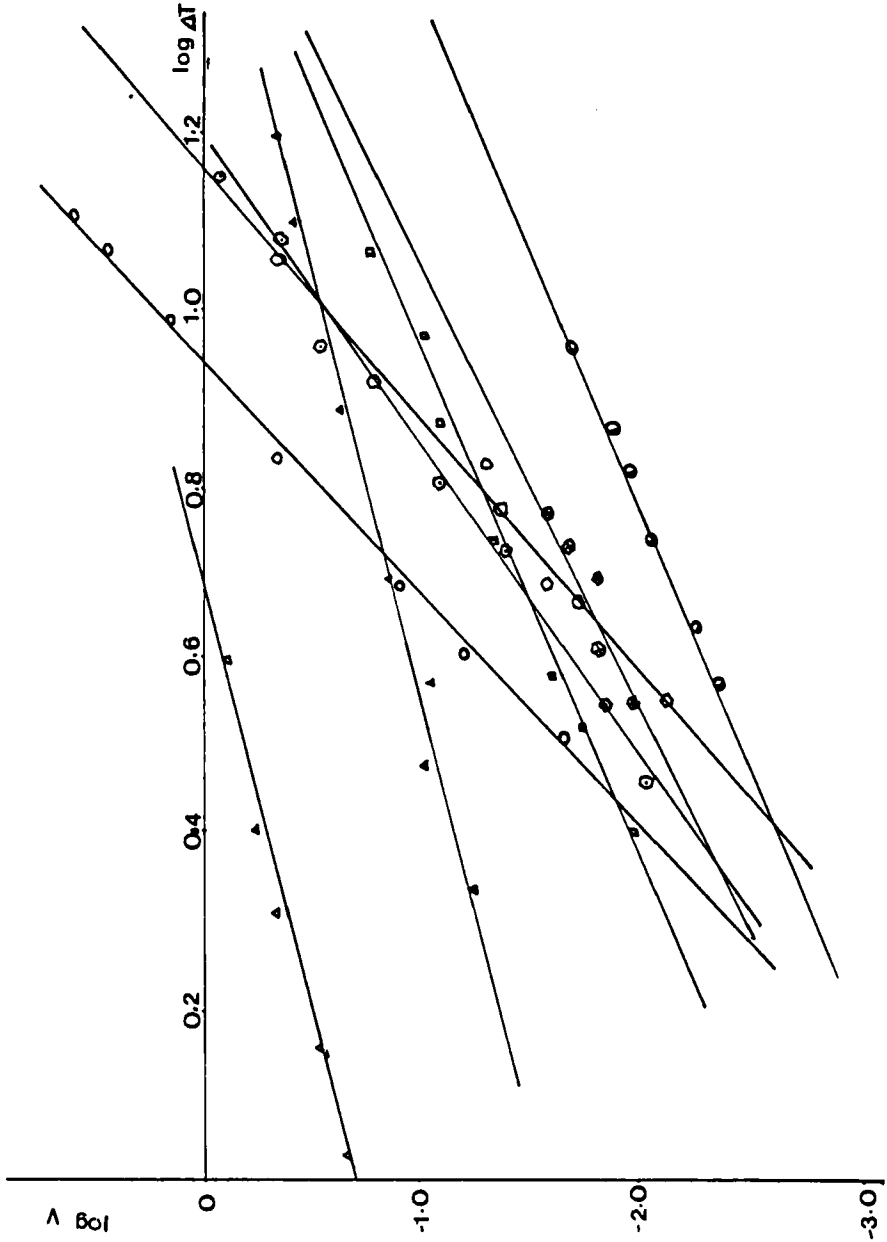

FIGURE 11 Linear Velocity of Crystallization of α · naphthol-β · naphthol-*m* · aminophenol system. ○ β · naphthol; ○ α · naphthol; *m* · aminophenol; α · naphthol-*m* · aminophenol eutectic; ▲ β · naphthol-*m* · aminophenol eutectic I; ■ β · naphthol-*m* · aminophenol eutectic II; ◐ α · naphthol-β · naphthol-*m* · aminophenol eutectic; △ α · naphthol · β · naphthol-*m* · aminophenol peritectic.

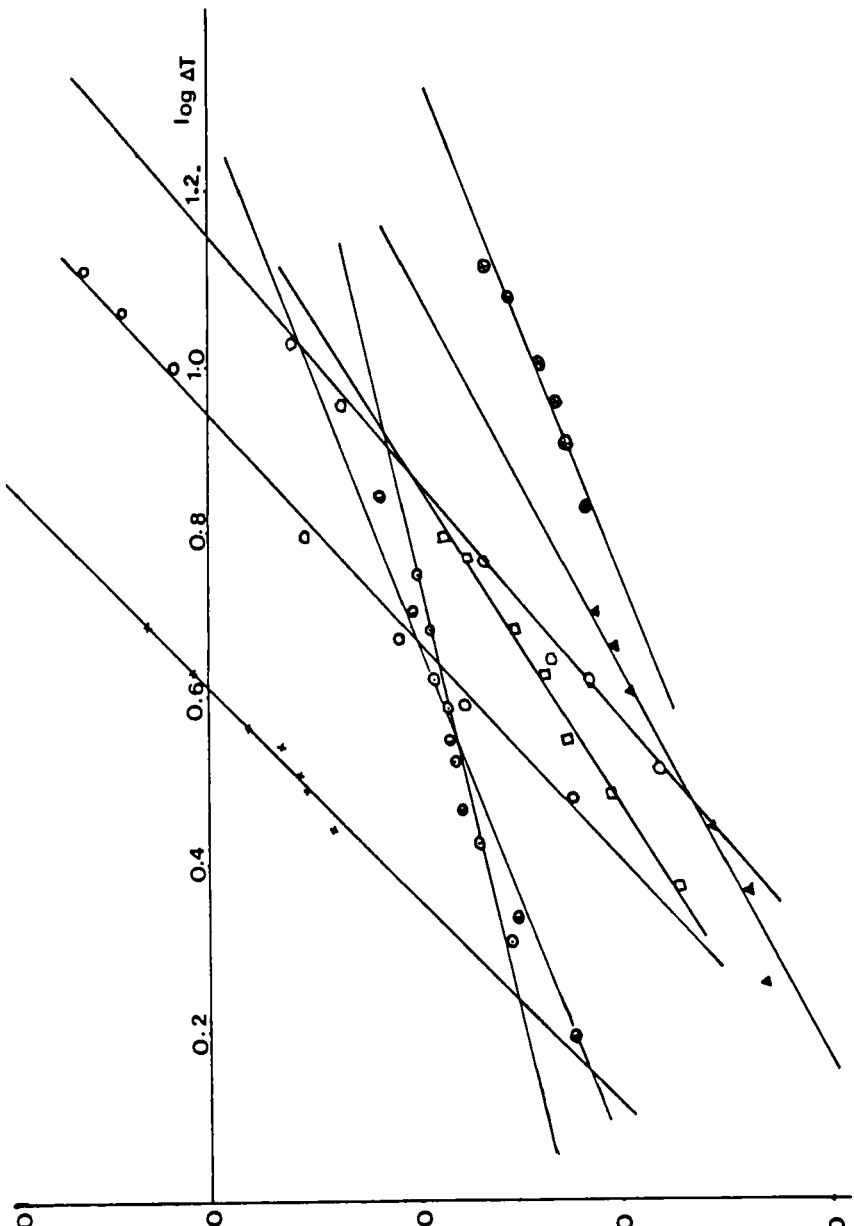

FIGURE 12 Linear Velocity of Crystallization of α·naphthol-β·naphthol-phenanthrene system. ○ α·naphthol; ○ β·naphthol; × phenanthrene; □ β·naphthol-phenanthrene eutectic; ▼ α·naphthol-phenanthrene eutectic I; ◐ α·naphthol-phenanthrene eutectic II; ⊗ α·naphthol-β·naphthol-phenanthrene eutectic; ⊙ α·naphthol-β·naphthol-phenanthrene peritectic.

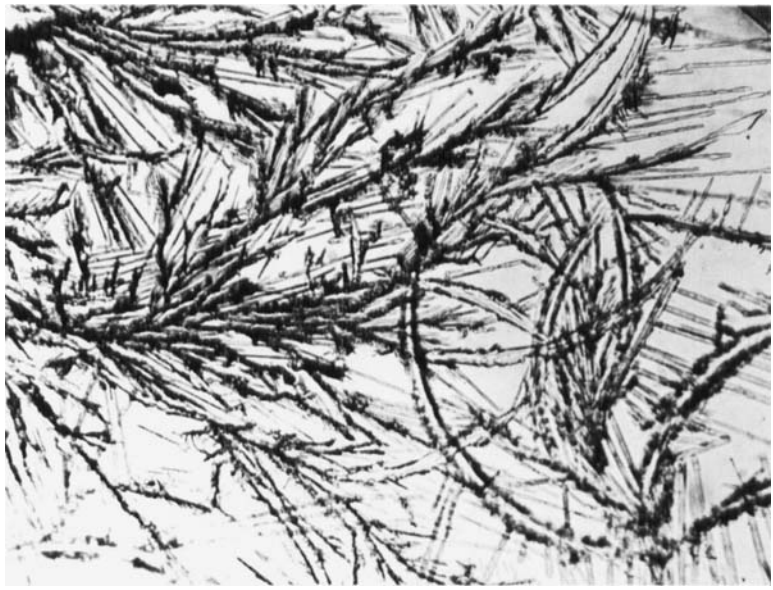

FIGURE 13 Microstructure of α·naphthol-*m*·aminophenol eutectic, ×50.

FIGURE 14 Microstructure of β·naphthol-phenanthrene eutectic, ×50.

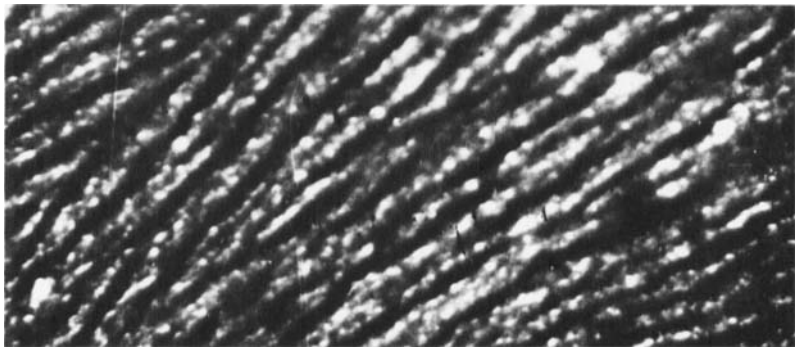

FIGURE 15 Microstructure of β-naphthol-*m*-aminophenol eutectic I, ×50.

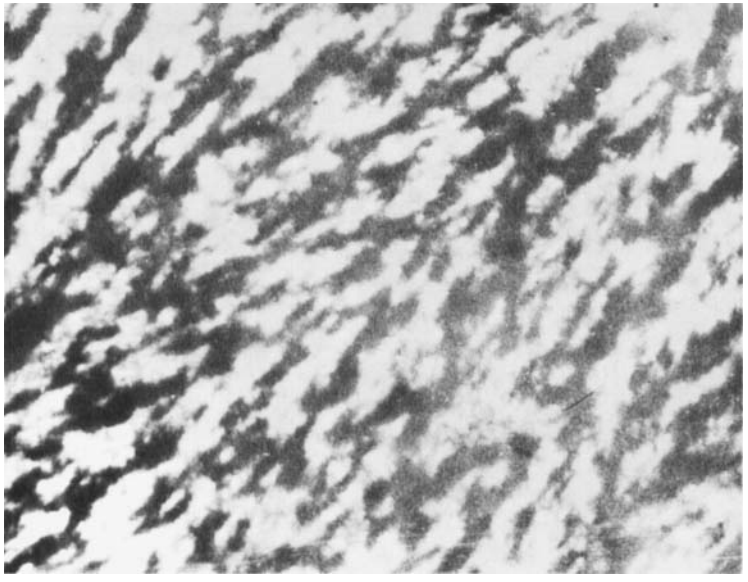

FIGURE 16 Microstructure of β-naphthol-*m*-aminophenol eutectic I, ×50 (high velocity).

The compositions theoretically predicted are given in Table II. The undercooling values are of the same order for the parent components as well as eutectics. This indicates, any of the phases of eutectic can nucleate the other. Since parent phases grew with approximately same undercoolings and same capacity of

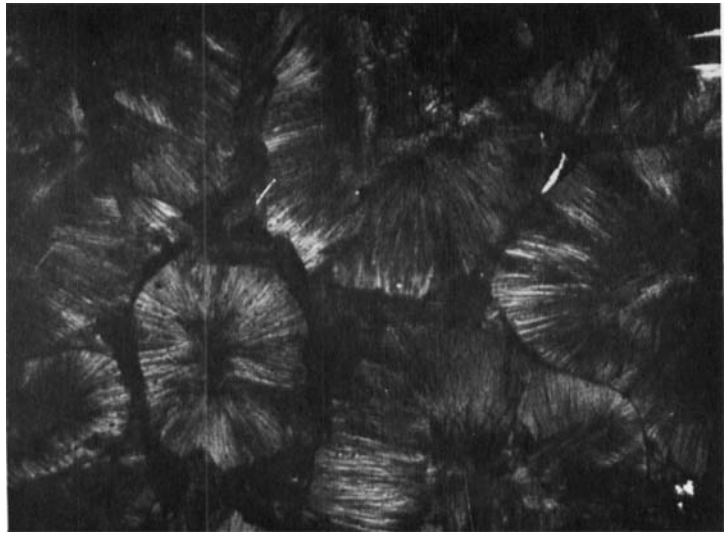

FIGURE 17 Microstructure of β-naphthol-*m*-aminophenol eutectic II, ×50.

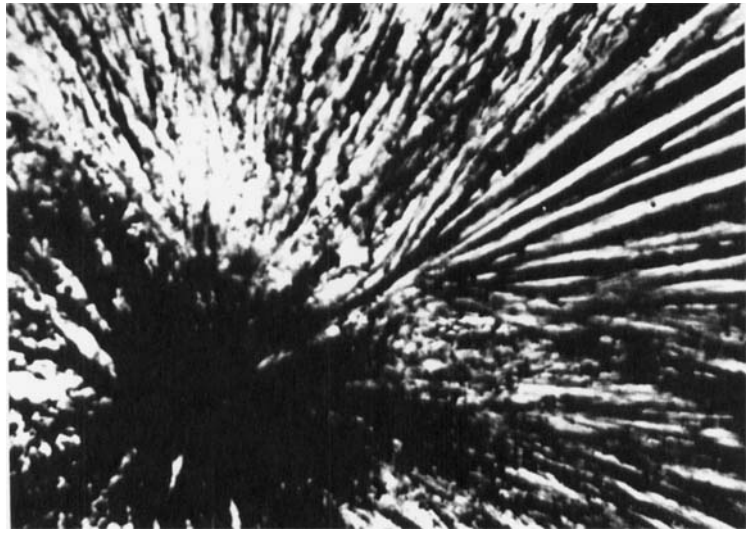

FIGURE 18 Microstructure of single nodul of β-naphthol-*m*-aminophenol eutectic II, ×50.

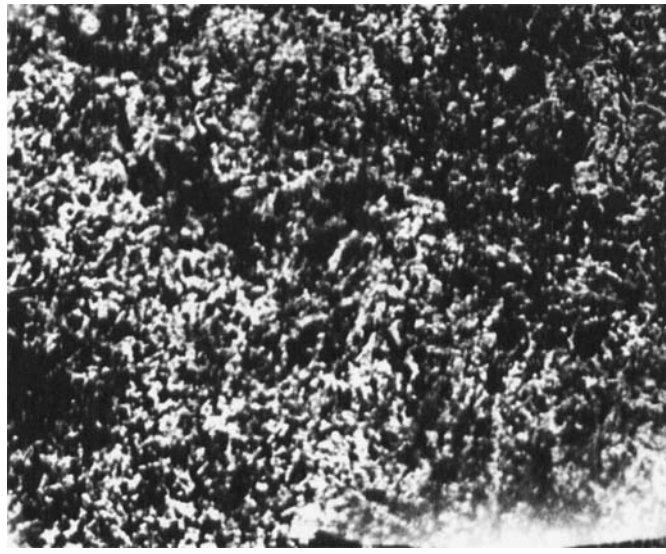

FIGURE 19 Microstructure of α-naphthol-phenathrene eutectic I, ×50.

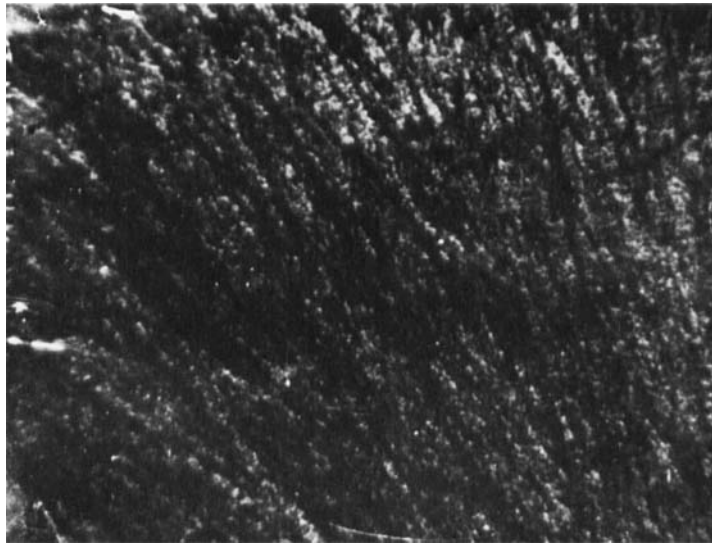

FIGURE 20 Microstructure of α-naphthol-phenathrene eutectic II, ×50.

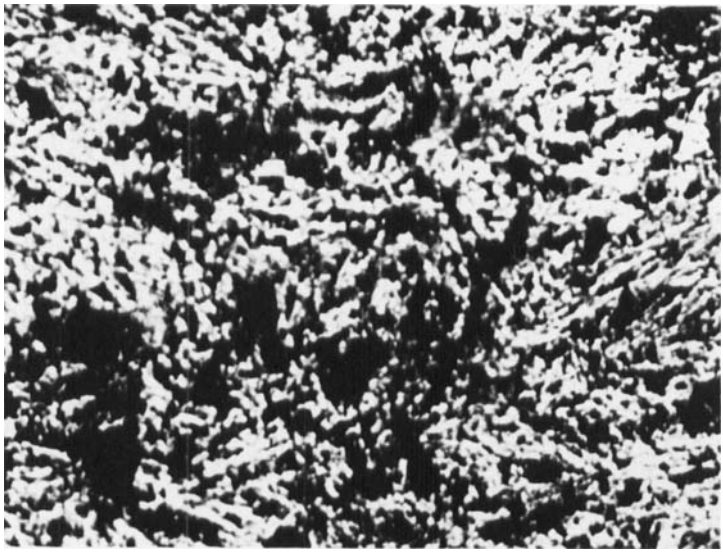

FIGURE 21 Microstructure of α·naphthol-β·naphthol-catechol eutectic, ×50.

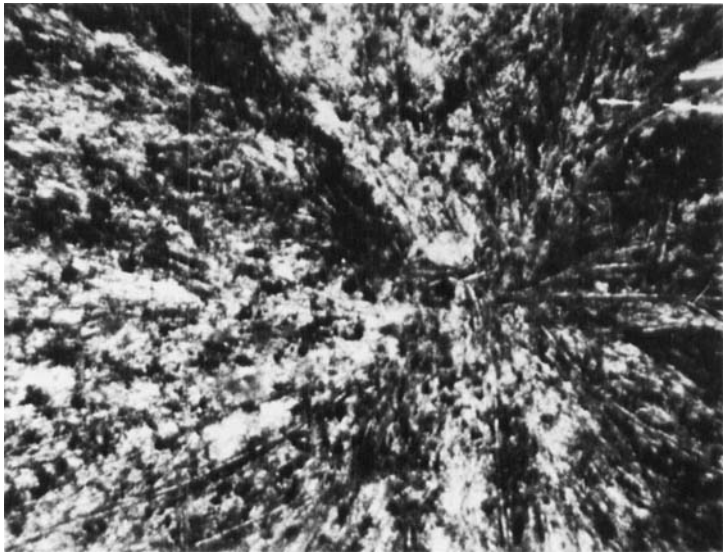

FIGURE 22 Microstructure of naphthalene-α·naphthol-cathechol eutectic, ×50.

FIGURE 23 Microstructure of α-naphthol-β-naphthol-phenanthrene eutectic, ×50.

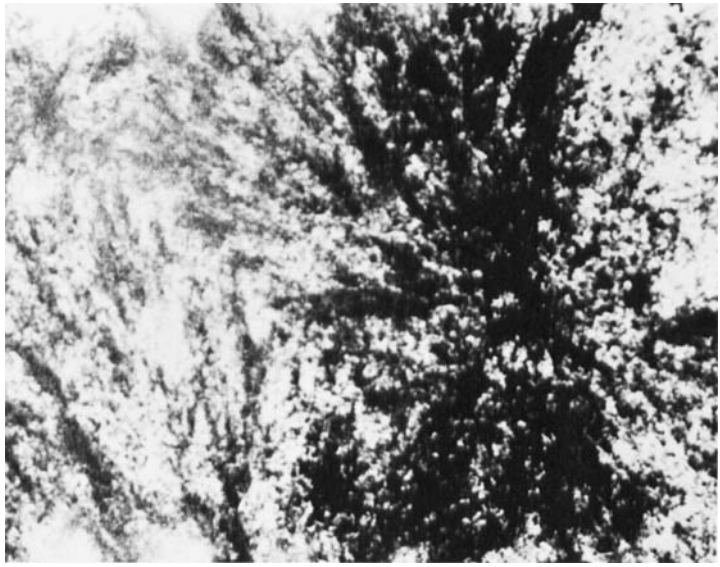

FIGURE 24 Microstructure of α-naphthol-β-naphthol-phenanthrene peritectic, ×50.

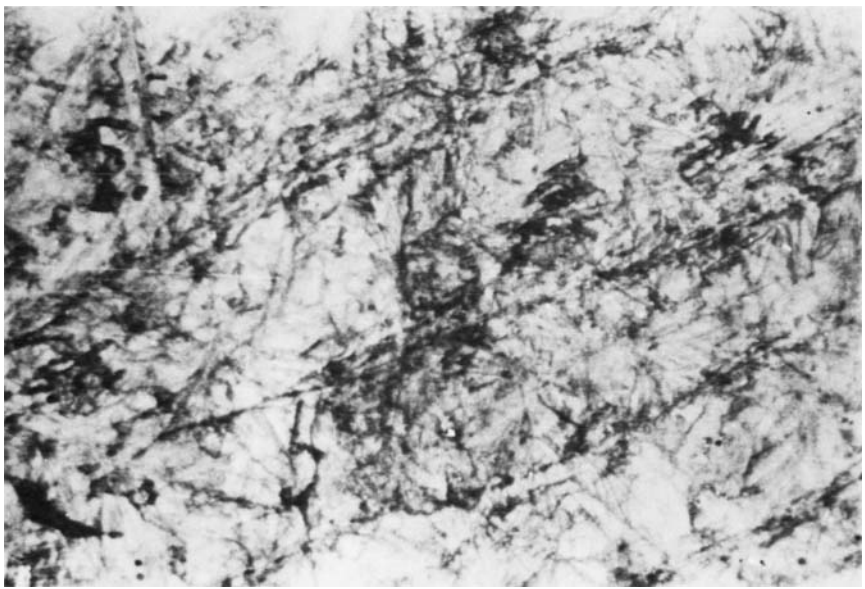

FIGURE 25 Microstructure of α·naphthol-β·naphthol-*m*·aminophenol eutectic, ×50.

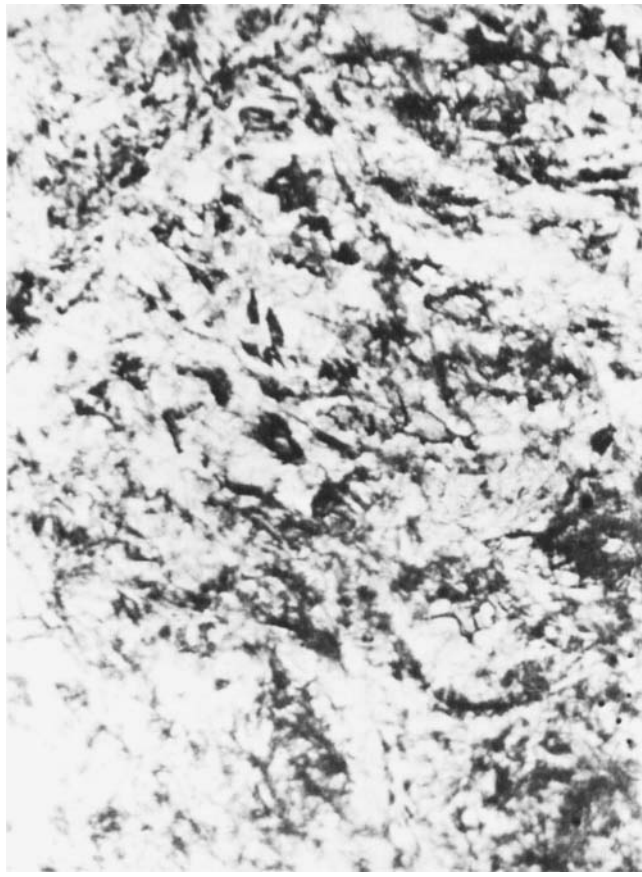

FIGURE 26 Microstructure of α·naphthol-β·naphthol-*m*·aminophenol peritectic. ×50.

TABLE IA

Experimental Heats of Fusion and Those Calculated from the Mixture Law for Binary Eutectics.

System	$(\Delta_f h)_e \times 10^{-2}$ J/M Exp.	$(\Delta_f h) \times 10^{-2}$ J/M	$(\Delta_f h)_e \times 10^{-2}$ J/M Calc.
α · naphthol-*m*·aminophenol	171.65	214.64	215.58
β · naphthol-phenanthrene	217.94	194.51	219.29
β · naphthol-*m*·aminophenol I	225.89	209.09	239.94
β · naphthol-*m*·aminophenol II	203.69	192.51	225.46
α · naphthol-phenanthrene I	207.36	205.34	229.04
α · naphthol-phenanthrene II	241.66	215.61	245.57

$(\Delta_f h) = X_1 \Delta_f h_1 + X_2 \Delta_f h_2$

and

$(\Delta_f h)_e = X_1 \Delta_f h_1 + X_2 \Delta_f h_2 + h^E$

TABLE IB

Comparison of Experimental Heats of Fusion and those Calculated from Mixture Law

System	$(\Delta_f h)_{exp} \times 10^{-2}$ J/M	$(\Delta_f h) \times 10^{-2}$ J/M
Naphthalene-α · naphthol-catechol	198.60	199.46
α · naphthol-β · naphthol-catechol	202.43	216.54
α · naphthol-β · naphthol-phenanthrene	203.00	203.48
α · naphthol-β · naphthol-*m*·aminophenol	211.43	215.67

TABLE II

Composition of Ternary Eutectics Calculated by Eq. 3.

System I	II	III	I m.f.	II m.f.	III m.f.
α · naphthol-β · naphthol-phenanthrene			0.3514	0.2309	0.4177
α · naphthol-β · naphthol-*m*·aminophenol			0.3928	0.2568	0.3504
α · naphthol-β · naphthol-catechol			0.3909	0.2561	0.3524
catechol-α · naphthol-naphthalene			0.2797	0.2564	0.4676

nucleating other phase, they overlapped or interspersed with one another during the growth. We shall discuss this topic in detail in sections of crystallization kinetics and microstructure.

(b) Crystallization kinetics

The rate at which growth occurs depend on the molecular mechanism of incorporation of molecules at crystal surface. Various theories[2-6,10] have been

developed for the growth mechanism of eutectics and predicted square relationship between crystallization velocity and undercooling. Experimentally, straight lines were obtained between log V and log ΔT, as per the following relationship.

$$V = \mu(\Delta T)^n \tag{4}$$

where μ and n are constant. The experimental values of these constants are given in Table III. The value of n for eutectics are approximately 2 in all the system. Although crystallization rates were low enough to assume that imposed ΔT was approximately same as ΔT at the interface, but slight deviations in values of n from 2 seem due to the difference between bath temperature and temperature of growing interface.

The crystallization behavior of simple eutectics (α · naphthol-m · aminophenol and β · naphthol-phenanthrene) can be discussed on the basis of Kofler's[11] idea of coupled growth. The parent phases were able to grow cooperatively by normal short range diffusional mechanism. When the parent phases nucleated within coupled zone, eutectic material engulfed the free dendrites of primary phases. Outside the coupled region it seems one primary phase first grew until surrounding liquid is enriched in other component to allow eutectic growth. Kinetic factors determine how this requirement affects the growth phenomena. The observed lower velocity of eutectic can be explained as follows: in α · naphthol-m · aminophenol eutectic, m · aminophenol nucleates from the melt more readily than α · naphthol. The growth of m · aminophenol crystals carries the composition of remaining melt away from

TABLE III

Values of n and μ for Eutectic Systems.

System	n	μmm sec^{-1} deg^{-1}
α · naphthol	3.56	0.00056
β · naphthol	3.60	0.00275
catechol	2.57	0.00055
naphthalene	1.88	1.51400
m · aminophenol	2.80	0.00083
phenanthrene	4.08	0.00263
α · naphthol-phenanthrene eutectic I	2.22	0.00055
α · naphthol-phenanthrene eutectic II	1.74	0.00791
β · naphthol-phenanthrene eutectic	1.81	0.00050
β · naphthol-m·aminophenol eutectic I	1.74	0.00020
β · naphthol-m·aminophenol eutectic II	1.80	0.00199
α · naphthol-β·naphthol-phenanthrene eutectic	1.74	0.00045
α · naphthol-β·naphthol-phenanthrene peritectic	1.25	0.01514
α · naphthol-β·naphthol-catechol eutectic	1.95	0.00033
α · naphthol-naphthalene-catechol eutectic	1.82	0.00166
α · naphthol-β · naphthol-m·aminophenol eutectic	1.77	0.00057
α · naphthol-β · naphthol-m · aminophenol peritectic	0.88	0.25120

the coupled zone and subsequent nucleation and growth of α · naphthol returns the melt composition to opposite direction. Thereafter both phases grow simultaneously from the melt, but being outside the coupled zone, they do not grow with equal velocity. Since crystals of *m* · aminophenol grow freely in the melt and α · naphthol nucleates repeatedly to consume remaining melt, the resulting microstructure consists of an intimate mixture of crystals, but lacks in regularlity. Similarly in β · naphthol-phenanthrene system, β · naphthol nucleates from the melt more readily than phenanthrene and crystallizes in a fashion similar to *m*-aminophenol-α · naphthol system.

The *m* · aminophenol-β · naphthol and α · naphthol-phenanthrene eutectics differ from the above eutectics in their crystallization behavior. In these systems 1:1 compounds are formed with congruent melting point. The growth rates of parent components and 1:1 compounds are higher than eutectics. The crystallization of eutectic e_1 (Figure 3) proceeds by side by side growth of β · naphthol and 1:1 compound. β · naphthol and 1:1 compound have approximately the same undercooling and melting temperature. When eutectic melt undercools, β · naphthol usually nucleates on 1:1 compound while composition remains in coupled zone, and phases growing at nearly equal velocity give normal (lamellar) structure. Eutectic e_2 crystallizes with the nucleation of *m* · aminophenol on 1:1 compound in coupled zone. Spherulites separate directly from the melt without simultaneous formation of any other solid. There is no true single interface, but there are many eutectic grains, which nucleate ahead of overall growth front and grow independently in the liquid. The pronounced tendency for undercooling during the solidification of eutectic spherulites together with large number of centers of growth suggest the lower growth rate as we found experimentally. The above picture can explain the lower growth velocity of phenanthrene-α · naphthol eutectics. In this system 1:1 compound has very low melting temperature than parent components. For eutectic e_1, phenanthrene and for e_2 α · naphthol nucleates to start the growth and 1:1 compound nucleates repeatedly to consume the remaining melt.

The crystallization with three independent constituents is more complex, but follows similar course of binary systems. The crystallization data for eutectics obey the square relationship ($n = 2$) as recently suggested by Hunt *et al.*[2] At all positions phases grew by the normal short range diffusional mechanism. Since parent–parent components are faceted, dividing line of the eutectic and parent phase is blurred and structural regions could not be well defined. α · naphthol-β · naphthol-catechol eutectic crystallized as three phase structure without any primary phase. Initially β · naphthol nucleates in the melt and catechol form coupled zone to crystallize binary eutectic, α · naphthol finally crystallizes cooperatively with β · naphthol-catechol eutectic. Naphthalene-α · naphthol-catechol also follows the same mechanism.

The crystallization behavior of α · naphthol-β · naphthol-*m* · aminophenol and α · naphthol-β · naphthol-phenathrene eutectic is very interesting due to existence of ternary peritectics (Figures 7 and 8). If we consider the solidification of peritectic *p*, *m* · aminophenol and β · naphthol) cannot separate simultaneously at this point. However, the only alternative is for some of *m* · aminophenol to redissolve in liquid to give α · naphthol and D, while temperature remains constant. When total *m* · aminophenol disappears, there are only three phases left so that temperature is free to drop along line $p\epsilon$ and depositing more α · naphthol and 1:1 compound of *m* · aminophenol and α · naphthol. When ternary eutectic *e* is reached, the temperature halts and residual liquid solidifies to give eutectic mixture of α · naphthol-β · naphthol and 1:1 compound of *m* · aminophenol and β · naphthol. In similar fashion ternary peritectic of α · naphthol-β · naphthol-phenanthrene crystallizes with redissolution of α · naphthol up to completion of ternary eutectic. At this point residual liquid solidifies to give mixture of phenanthrene, β · naphthol and 1:1 compound of α · naphthol-phenanthrene. This picture shows that growth velocity of peritectic will not be lower than binary eutectics as have been observed in the present systems.

(c) Heat of fusion

The experimentally determined values of heat of fusion are given in Table I. In the same table values calculated by mixture law are also reported. If the eutectic is assmed to be a mechanical mixture involving no heat of mixing, the heat of fusion will be given by the relationship:

$$(\Delta_f h) = \sum X_i \Delta_f h_i \tag{5}$$

It has been observed that the enthalpy changes on mixing so this mixture law is not obeyed. Excess thermodynamic functions were calculated as in Ref. 5. The values computed by the mixture law are much higher than the experimentally determined values, indicating that association occurs in the melt.

The experimentally determined values of the heat of fusion were compared with values computed by empirical equations for binary and ternary eutectics.

$$(\Delta_f h)_e = \frac{k\, T_e^2}{X_1 T_{b_1} + X_2 T_{b_2}} \tag{6}$$

and

$$(\Delta_f h)_e = \frac{k\, T_e^2}{X_1 T_{b_1} + X_2 T_{b_2} + X_3 T_{b_3}} \tag{7}$$

where k is a constant equal to 0.175, T_e is the eutectic temperature in K, X_i and T_{bi} are mole fraction and normal boiling point in K of component i. These values

are given in Tables IV and V for binary and ternary eutectics and agree well with experimental values.

(d) Microstructure

The microstructure of α · naphthol-*m* · aminophenol eutectic is dentritic (Figure 13). It appears that both components grew side by side from left to right. β · naphthol-phenanthrene eutectic is irregularly arranged (Figure 14) in the form of dark spots interspersed on white background. The dark spots are eutectic grains. First eutectic of β · naphthol-*m* · aminophenol (0.31 mole fraction of *m* · aminophenol) has parallel twin structure. The simultaneous solidification of constituent phases impose restriction on nucleation and growth that has no counterpart in single phase solidification. Because of independent nature of the growth of phases, cross diffusion ahead of the interface, phases could not escape one from the influence of the other. Second eutectic (Figure 17) is nodular. On microscopic scale nodules consist of lamellas of constituent phases radiating outward from its center, and growing approximately normal to solid–liquid interface. The eutectic solidifies in all directions at a uniform rate and the interface between eutectic nodule and melt is quite sharp on lamellar scale. Figure 18 shows microstructure at high magnification. The nu-

TABLE IV

Activity Coefficients of Components in Binary Liquid Eutectics

System I	System II	log γ_1	log γ_2
α · naphthol-*m*·aminophenol		−0.1064	0.1740
β · naphthol-phenanthrene		0.0956	0.0369
α · naphthol-phenanthrene eutectic I		0.0151	0.0233
α · naphthol-phenanthrene eutectic II		−0.1871	0.1791
β · naphthol-*m*·aminophenol eutectic I		−0.0770	0.4257
β · naphthol-*m*·aminophenol eutectic II		0.18180	0.0870

TABLE V

Excess Thermodynamic Functions for Binary Eutectics

System	$h^E \times 10^{-2}$ *J/M*	$g^E \times 10^{-1}$ *J/M*	s^E *J/M* °K
α · naphthol-*m*·aminophenol eutectic	0.93	34.96	0.32
β · naphthol-phenanthrene eutectic	24.78	9.27	6.94
α · naphthol-phenanthrene eutectic I	23.70	3.10	8.75
α · naphthol-phenanthrene eutectic II	29.96	−9.12	5.86
β · naphthol-*m*·aminophenol eutectic I	30.48	9.16	8.96
β · naphthol-*m*·aminophenol eutectic II	32.94	21.47	8.63

TABLE VI

Heats of Fusion Calculated by Eq. 6 for Binary Eutectics and Eq. 7 for Ternary Eutectics

System	Heats of Fusion Calculated by Eqs. 11 and 12 cal/gm	Experimental Heats of Fusion. cal/gm
α · naphthol-*m*·aminophenol	35.08	31.54
β · naphthol-phenanthrene	36.35	32.07
α · naphthol-phenanthrene I	34.09	31.40
α · naphthol-phenanthrene II	33.84	37.07
β · naphthol-*m*·aminophenol I	42.80	41.30
β · naphthol-*m*·aminophenol II	43.29	40.47
naphthalene-catechol-α · naphthol	35.19	36.58
α · naphthol-β · naphthol-*m*·aminophenol	35.16	35.76
α · naphthol-β · naphthol-catechol	34.09	36.35
α · naphthol-β · naphthol-phenanthrene	31.67	35.07

cleation center and both phases are clearly visible in microstructure. The microstructure of α · naphthol-phenanthrene I (0.42 mole fraction of α · naphthol) is rod type (Figure 19) and II (0.64 mole fraction of α · naphthol) is lamellar (Figure 20) type.

α · naphthol-β · naphthol-catechol ternary eutectic has Chinese script (Figure 21) type microstructure. Two phases grew side by side and third is interspersed in such a way that whole structure seems to be regular. Naphthalene-α · naphthol-catechol eutectic is feather type (Figure 22). Phases grow side by side away from nucleation center. The growth rate of naphthalene is higher than α · naphthol as well as catechol so it grows rapidly affecting the interface which changes to fanlike structure. From Figure 23 it appears that all three phases of α · naphthol-β · naphthol-*m* · aminophenol eutectic and peritectic are shown in Figures 25 and 26. Eutectic is cellular in which cells seem to be changing to dendrites. The phases are irregularly distributed on growth plane.

Acknowledgments

The financial support by the State Council of Science and Technology U.P. India is gratefully acknowledged.

References

1. G. J. Sloan and A. R. McGhie, *J. Crystal Growth,* **32,** 60 (1976).
2. D. G. McCartney, J. D. Hunt and R. M. Jordan, *Trans. Met. Soc. AIME,* **11A,** 1243 (1980).
3. W. Kurz and D. J. Fischer, *Acta Met.,* **28,** 777 (1980).
4. B. Chalmers, "Principles of Solidification", John Wiley and Sons, New York, 1964.
5. K. A. Jackson and J. D. Hunt, *Trans. Met. Soc. AIME,* **236,** 1129 (1966).

6. R. P. Rastogi, N. B. Singh, P. Rastogi and Narsingh Bahadur Singh, *J. Crystal Growth*, **40**, 329 (1977).
7. R. P. Rastogi, N. B. Singh and Narsingh Bahadur Singh, *J. Crystal Growth*, **37**, 234 (1977).
8. Narsingh Bahadur Singh, Ph.D. Thesis, University of Gorakhpur, India, 1976.
9. N. B. Singh and Narsingh Bahadur Singh, *J. Crystal Growth*, **28**, 267 (1975).
10. M. E. Glicksman, "Direct Observation on Solidification", edited by T. J. Haughel, ASM, Ohio 1971.
11. A. Kofler, *Z. fur Electrochem*, **57**, 721 (1953).
12. G. A. Chadwick, "Solidification of Metals", 138, ISI, 1967.